A tandem queue with coupled processors: computational issues

J.S.H. van Leeuwaarden
EURANDOM,
P.O. Box 513, 5600 MB Eindhoven, The Netherlands
e-mail: j.s.h.v.leeuwaarden@tue.nl

J.A.C. Resing
Eindhoven University of Technology,
Department of Mathematics and Computer Science,
P.O. Box 513, 5600 MB Eindhoven, The Netherlands
e-mail: j.a.c.resing@tue.nl

February 2004

Abstract

In [13] it is shown that the two-stage tandem queue with coupled processors can be solved using the theory of boundary value problems. In this paper we consider the issues that arise when calculating performance measures like the mean queue length and the fraction of time a station is empty.

It is assumed that jobs arrive at the first station according to a Poisson process and require service at both stations before leaving the system. The amount of work that a job requires at each of the stations is an independent, exponentially distributed random variable. When both stations are nonempty, the total service capacity is shared among the stations according to fixed proportions. When one of the stations becomes empty, the total service capacity is given to the nonempty station.

We study the two-dimensional Markov process representing the numbers of jobs at the two stations. The problem of finding the generating function of the stationary distribution can be reduced to two different Riemann-Hilbert boundary value problems. Although both problems yield a complete analytical solution, from the numerical viewpoint they have different features. We discuss the similarities and differences between the two problems, and relate them to the computational aspects of obtaining performance measures.

1 Introduction

Consider a two-stage tandem queue, where jobs arrive at the first station according to a Poisson process. After receiving service at this station, they move to the second station, and upon completion of service at the second station they leave the system. The amount of work that a job requires at each of the stations is an exponentially distributed random variable, and the total service capacity of the two stations together is constant. When both stations are nonempty, a given proportion of the capacity is allocated to station 1, and the remaining

proportion is allocated to station 2. If one of the stations is empty, however, the total service capacity of the stations is allocated to the nonempty station.

The model is motivated by a situation that arises in cable TV networks which have been upgraded to enable bidirectional communications between users and a centrally located head end (HE). In order to coordinate transmissions from users to HE a medium access protocol is needed. This protocol can be a mechanism consisting of two stages. At the first stage, a user which has data to transmit sends a request to the HE in a dedicated time slot to specify the number of data slots it needs. If only one user sends a request in a certain time slot, the HE receives the request successfully. If more users simultaneously send a request in a certain time slot, a collision occurs, upon which a collision resolution algorithm is started for these users. Upon receiving a request successfully, the HE starts the second stage of the mechanism, the actual data transmission, by sending a grant to the corresponding user to transmit its data in specified data slots. The capacity of the channel is divided between these two stages by using each time slot to either transmitting data of users already having a grant or handling requests of users not yet having a grant. Clearly, in our model, service at station 1 represents the process of sending the requests, whereas service at station 2 represents the transmission of the actual data corresponding to the successfully received requests.

Another application of the model would be an assembly line for which on each job two operations must be performed using a limited service capacity. By coupling the service at each of the operations, and thus using the service capacity of an operation for which no jobs are waiting for the other operations, imbalance in the assembly line can be reduced and the throughput can be increased (see e.g. Andradottir et al. [1]).

Resing and Örmeci [13] have shown for the two-dimensional Markov process representing the numbers of jobs at the two stations, that the problem of finding the bivariate generating function of the stationary distribution can be reduced to a Riemann-Hilbert boundary value problem. The theory of boundary value problems was introduced to the field of queueing theory by Fayolle and Iasnogorodski [6], who analyzed two coupled processors in parallel with exponential service times. Some years later, the book of Cohen and Boxma [5] made the technique of solving queueing systems with boundary value problems into an established one.

In [13] the issue how to obtain performance measures has not been discussed. In general, obtaining performance measures from the formal solution of a Riemann-Hilbert boundary value problem is not straightforward. In this paper we discuss the numerical issues that arise when obtaining performance measures. In particular, we consider the fraction of time a station is empty and the mean stationary queue length at a station. The reduction of the problem of finding the generating function to a boundary value problem usually follows from considering a specific zero-set of the kernel of the functional equation. This can be done in more than one way. We discuss, next to the zero-set in [13], one other zero-set that leads to a second Riemann-Hilbert boundary value problem. From the analytical viewpoint, the second model has little added value, since solving either one of the two problems gives a full solution to the model. However, in determining performance measures numerically the two problems have different features.

We describe the model and the key functional equation for the model in Section 2 and 3. The reduction of the problem of finding the stationary queue length distribution of the model to a Riemann-Hilbert boundary value problem, as introduced in [13], is described in Section 4.1 and 5. In Section 4.2 and 6 we introduce the second Riemann-Hilbert boundary value problem. In particular, in Section 6.1 attention is paid to determining the conformal map that is required for the solution of the second Riemann-Hilbert boundary value problem. In

Section 7 we derive some performance measures for the model. In Section 8 we discuss issues that arise when numerically determining the performance measures from the formal solutions of the Riemann-Hilbert boundary value problems. Among other things, we show in Section 8.2 that we can determine the performance measures for the whole set of allowed parameter values. Finally, we give some numerical results in Section 9.

2 Model description

Consider a two-stage tandem queue, where jobs arrive at queue 1 according to a Poisson process with rate λ, each job demanding service at both queues before leaving the system. Each job requires an exponential amount of work with parameter ν_j at station j, $j = 1, 2$. The total service capacity of the two service stations together is fixed. Without loss of generality we assume that this total service capacity equals one unit of work per time unit. Whenever both stations are nonempty, a proportion p of the capacity is allocated to station 1, and the remaining part $1 - p$ is allocated to station 2. Thus, when there is at least one job at each station, the departure rate of jobs at station 1 is $\nu_1 p$ and the departure rate of jobs at station 2 is $\nu_2(1-p)$. Here we assume that $0 < p < 1$, so that there is a real capacity sharing among the two processors. For the cases $p = 0$ and $p = 1$, the system can be seen as a tandem queue with a single server moving between the two queues and giving priority to one of the queues. The solutions for these cases are given in [13].

When one of the stations becomes empty, the total service capacity is allocated to the nonempty station. Hence, the departure rate at that station, station j say, is temporarily increased to ν_j. With $X_j(t)$ the number of jobs at station j at time t, the two-dimensional process $\{(X_1(t), X_2(t)), t \geq 0\}$ is a Markov process. The ergodicity condition under which this Markov process has a unique stationary distribution is given by

$$\frac{\lambda}{\nu_1} + \frac{\lambda}{\nu_2} < 1. \tag{2.1}$$

This can be explained by the fact that, independent of p, the two stations together always work at capacity 1 (if there is work in the system), and that $\lambda/\nu_1 + \lambda/\nu_2$ equals the amount of work brought into the system per time unit. We henceforth assume that the ergodicity condition is satisfied.

3 Functional equation

Let us denote by $\pi(n, k)$ the stationary probability of having n customers at station 1 and k customers at station 2, i.e. $\pi(n, k) = \lim_{t\to\infty} \mathbb{P}(X_1(t) = n, X_2(t) = k)$. The following set of balance equations can then be derived:

$$\begin{aligned}
\lambda\pi(0,0) &= \nu_2\pi(0,1), \\
(\lambda+\nu_1)\pi(n,0) &= \lambda\pi(n-1,0) + (1-p)\,\nu_2\pi(n,1), \quad n \geq 1, \\
(\lambda+\nu_2)\pi(0,1) &= \nu_1\pi(1,0) + \nu_2\pi(0,2), \\
(\lambda + p\,\nu_1 + (1-p)\,\nu_2)\pi(n,1) &= \lambda\pi(n-1,1) + \nu_1\pi(n+1,0) + (1-p)\,\nu_2\pi(n,2), \quad n \geq 1, \\
(\lambda+\nu_2)\pi(0,k) &= p\,\nu_1\pi(1,k-1) + \nu_2\pi(0,k+1), \quad k \geq 2, \\
(\lambda + p\,\nu_1 + (1-p)\,\nu_2)\pi(n,k) &= \lambda\pi(n-1,k) + p\,\nu_1\pi(n+1,k-1) + (1-p)\,\nu_2\pi(n,k+1), \\
&\qquad n \geq 1, \quad k \geq 2.
\end{aligned}$$

We define the joint probability generating function

$$P(x,y) := \sum_{n\geq 0}\sum_{k\geq 0} \pi(n,k)x^n y^k, \quad |x|\leq 1,\ |y|\leq 1,$$

which is, for every fixed y, regular for $|x|<1$ and continuous for $|x|\leq 1$. A similar statement holds for the role of x and y interchanged. From the balance equations it follows that $P(x,y)$ satisfies the functional equation

$$h_1(x,y)P(x,y) = h_2(x,y)P(x,0) + h_3(x,y)P(0,y) + h_4(x,y)P(0,0), \tag{3.1}$$

where

$$\begin{aligned}
h_1(x,y) &:= (\lambda + p\,\nu_1 + (1-p)\,\nu_2)xy - \lambda x^2 y - p\,\nu_1 y^2 - (1-p)\,\nu_2 x,\\
h_2(x,y) &:= (1-p)\,[\nu_1\, y(y-x) + \nu_2\, x(y-1)],\\
h_3(x,y) &:= p\,[\nu_2\, x(1-y) + \nu_1\, y(x-y)],\\
h_4(x,y) &:= p\,\nu_2\, x(y-1) + (1-p)\,\nu_1\, y(x-y).
\end{aligned}$$

The constant $P(0,0)$ can be determined by substituting $x=\gamma(y) := \nu_1 y^2/(\nu_1 y - \nu_2 y + \nu_2)$ into (3.1). For this choice of x, both $h_2(x,y)$ and $h_3(x,y)$ equal zero, and hence (3.1) reduces to

$$P(\gamma(y),y) = \frac{h_4(\gamma(y),y)}{h_1(\gamma(y),y)}P(0,0). \tag{3.2}$$

Letting $y\uparrow 1$ in (3.2), we obtain $P(0,0) = 1-\lambda/\nu_1-\lambda/\nu_2$. This result can again be explained by the fact that, independent of p, the two stations together always work at capacity 1 (if there is work in the system), and that $\lambda/\nu_1+\lambda/\nu_2$ equals the amount of work brought into the system per time unit.

4 Analysis of the kernel

In the analysis of the functional equation (3.1) a crucial role is played by the kernel $h_1(x,y)$. Due to the regularity properties of $P(x,y)$, for each pair (x,y) on or within the unit circle for which $h_1(x,y)$ equals zero, the right-hand side of (3.1) must vanish. This provides us with a relation between the unknown functions $P(0,y)$ and $P(x,0)$. From the observation that $h_1(x,y)$ is a polynomial in either x or y, we can construct two Riemann-Hilbert boundary value problems, one for the function $P(x,0)$ and one for the function $P(0,y)$.

Blanc [2] has investigated the transient behavior of the ordinary tandem queue without coupled processors, for which the kernel $h_1(x,y)$ is of the exact same form. Since Blanc has studied $h_1(x,y)$ as a polynomial in y, most of the results presented in Section 4.1 stem from his work. Using these results, the problem of finding the stationary queue length distribution can be reduced to a Riemann-Hilbert boundary value problem for $P(0,y)$, as presented in [13] and Section 5 of this paper. In Section 4.2 we present results concerning $h_1(x,y)$ as a polynomial in x, from which we derive a Riemann-Hilbert boundary value problem for $P(x,0)$ in Section 6.

4.1 $h_1(x, y)$ as a polynomial in y

We introduce

$$r_1 = \frac{\lambda}{p\nu_1}, \quad r_2 = \frac{\lambda}{(1-p)\nu_2},$$

as the loads on each of the stations during periods when both stations are nonempty. For notational convenience, we also introduce

$$\hat{r} = 1 + \frac{1}{r_1} + \frac{1}{r_2},$$

such that

$$h_1(x, y) = \lambda\Big[\hat{r}xy - x^2y - \frac{1}{r_1}y^2 - \frac{1}{r_2}x\Big]. \tag{4.1}$$

Observe that $h_1(x, y)$ is, for each x, a polynomial of degree 2 in y. We thus have that for every value of x there are two possible values of y, say $y_1(x)$ and $y_2(x)$, such that $h_1(x, y_1(x)) = h_1(x, y_2(x)) = 0$. These can be described by the two-valued function

$$y(x) = \frac{r_1}{2}[s_1(x) \pm \sqrt{D_1(x)}], \tag{4.2}$$

where

$$s_1(x) = (\hat{r} - x)x, \quad D_1(x) = s_1(x)^2 - \frac{4x}{r_1 r_2}.$$

We then obtain the following result:

Lemma 4.1. *The algebraic function $y(x)$, defined by $h_1(x, y(x)) = 0$, has four real branch points $0 = x_1 < x_2 \leq 1 < x_3 < x_4$.*

Proof: The branch points of $y(x)$ are zeros of the discriminant $D_1(x)$. Clearly, $D_1(0) = 0$, $\lim_{x\downarrow 0} D_1(x) < 0$, $D_1(1) \geq 0$, $D_1(\hat{r}) < 0$ and $\lim_{x\to\infty} D_1(x) = \infty$. Furthermore, if $D_1(1) = 0$ (i.e. $r_1 = r_2 < 1$) then $D'(1) > 0$. □

For later use, we now study the mapping $y(x)$ for $x \in [0, x_2]$ in some more detail. This mapping can be shown to give rise to a smooth and closed contour L, as specified in the next lemma, and illustrated in Figure 1.

Lemma 4.2. *For each $x \in [0, x_2]$, $y(x)$ lies on the closed contour L, which is symmetric with respect to the real line, and defined by:*

$$|y|^2 = \frac{r_1}{2r_2}(\hat{r} - \sqrt{\hat{r}^2 - 8\mathrm{Re}(y)/r_1}), \tag{4.3}$$

$$|y|^2 \leq \frac{r_1}{r_2}x_2. \tag{4.4}$$

Proof: For $x \in [0, x_2]$, $D_1(x)$ is negative, so $y_1(x)$ and $y_2(x)$ are complex conjugates. It also follows that

$$\mathrm{Re}(y) = \frac{r_1}{2}(\hat{r} - x)x. \tag{4.5}$$

Furthermore, from $h_1(x, y(x)) = 0$ we have $|y|^2 = r_1x/r_2 \leq r_1x_2/r_2$. Since (4.5) is a quadratic equation in x, substituting one of the two solutions into $|y|^2 = r_1x/r_2$ yields (4.3).

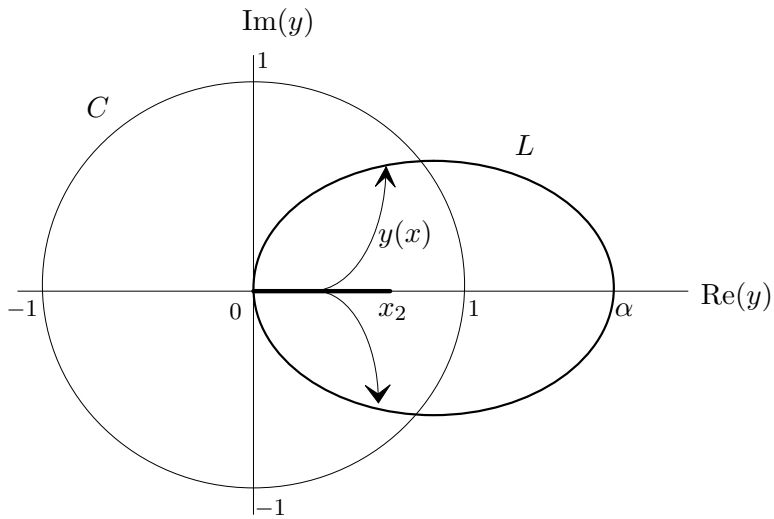

Figure 1: The mapping $y = y(x) : [0, x_2] \to L$.

Of course, we choose the solution of x for which $y(0) = 0$ and $y(x_2) = \sqrt{r_1 x_2/r_2}$ lie on the contour. □

We will henceforth denote the interior of L by L^+, and set

$$\alpha := y(x_2) = \sqrt{r_1 x_2/r_2}, \tag{4.6}$$

representing the point on L with the largest modulus. With respect to α, the following assertions hold.

Lemma 4.3. *If $r_1 = r_2$, then $\alpha = 1$. If $r_1 < r_2$, then $\alpha < 1$. If $r_1 > r_2$, then $\alpha > 1$.*

Proof: For $r_1 = r_2$, we have that $D_1(1) = 0$, so $x_2 = \alpha = 1$. For $r_1 < r_2$, knowing $x_2 < 1$, it follows that $\alpha < 1$. For $r_1 > r_2$, knowing $x_2 < 1$, we have that $D_1(r_2/r_1) < 0$ since $r_2 + r_2(1 - r_2)/r_1 < 1$, and thus $r_2/r_1 < x_2$ and $\alpha > 1$. □

We note that $\alpha = 1$ (resp. $\alpha < 1$, $\alpha > 1$) implies $1 \in L$ (resp. $1 \notin L \cup L^+$, $1 \in L^+$), which plays a crucial role in the numerical work to be presented in Section 8. We will elaborate on this in Section 8.1.

4.2 $h_1(x, y)$ as a polynomial in x

Paralleling the approach in Section 4.1, the kernel $h_1(x, y)$ is, for each y, a polynomial of degree 2 in x. Thus for each y there are two possible values of x, say $x_1(y)$ and $x_2(y)$, such that $h_1(x_1(y), y) = h_1(x_2(y), y) = 0$. These can be described by the two-valued function

$$x(y) = \frac{1}{2y}[s_2(y) \pm \sqrt{D_2(y)}], \tag{4.7}$$

where

$$s_2(y) = \hat{r}y - \frac{1}{r_2}, \quad D_2(y) = s_2(y)^2 - \frac{4y^3}{r_1}.$$

The following then holds:

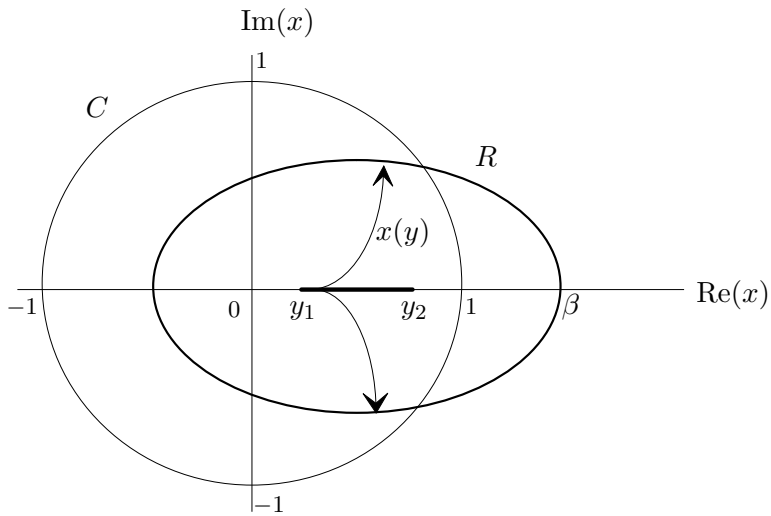

Figure 2: The mapping $x = x(y) : [y_1, y_2] \to R$.

Lemma 4.4. *The algebraic function $x(y)$ defined by $h_1(x(y), y) = 0$ has three real branch points $0 < y_1 < y_2 \leq 1 < y_3$.*

Proof: The branch points of $x(y)$ are zeros of the discriminant $D_2(y)$. Clearly, $D_2(0) = 1/r_2^2 > 0$, $D_2(1) = (1 - 1/r_1)^2 \geq 0$ and $\lim_{y\to\infty} D_2(y) = -\infty$. For $\hat{y} = 1/(r_2\hat{r}) \in (0, 1)$, it holds that $D_2(\hat{y}) = -4\hat{y}^3/r_1 < 0$. Furthermore, if $D_2(1) = 0$ (i.e. $r_1 = 1$ and, due to the ergodicity condition, $r_2 < 1$) then $D_2'(1) = 4(1/r_2 - 1) > 0$. □

We now study the mapping $x(y)$ for $y \in [y_1, y_2]$ in some more detail. This mapping can be shown to give rise to a smooth and closed contour R, as specified in the next lemma and illustrated in Figure 2.

Lemma 4.5. *For each $y \in [y_1, y_2]$, $x(y)$ lies on the closed and smooth contour R, which is symmetric with respect to the real line, and defined by:*

$$|x|^2 = \frac{1}{r_1 r_2(\hat{r} - 2\mathrm{Re}(x))}, \tag{4.8}$$

$$|x|^2 \leq \frac{y_2}{r_1}. \tag{4.9}$$

Proof: Similar to the proof of Lemma 4.2. □

We set

$$\beta := x(y_2) = \sqrt{y_2/r_1}, \tag{4.10}$$

the point on R with the largest modulus, for which it holds that

Lemma 4.6. *(i) When either $r_1 = 1$ or $r_2 = 1$ we have that $\beta = 1$. (ii) When both $r_1 < 1$ and $r_2 < 1$ we have that $\beta > 1$. (iii) When either $r_1 > 1$ or $r_2 > 1$ we have that $\beta < 1$.*

Proof: (i) If $r_1 = 1$, then $y_2 = 1$ and thus $\beta = 1$. If $r_2 = 1$, then $y_2 = r_1$ and thus $\beta = 1$.

(ii) For $\beta > 1$ we should prove that $r_1 < y_2$. Consider the function $f(r_1) := D_2(r_1) = -4r_1^2 + (1 + r_1 + r_1/r_2 - 1/r_2)^2$. The solutions to $f(r_1) = 0$ are given by $r_1 = 1$ and $r_1 = \hat{r}_1 = (1-r_2)/(1+3r_2)$. For $r_1 = \hat{r}_1$ it holds that $r_1 = y_1 < y_2$. Assume that there exists a value $r_1 \in (0,1)$ for which it holds that $r_1 > y_2$. Then, since y_2 is a continuous function of r_1, there should be a value in $(0,1)$ other than $\hat{r}_1$ for which $r_1 = y_2$ and hence $f(r_1) = 0$. This is not the case, and thus $r_1 < y_2$ for all values $r_1 \in (0,1)$.

(iii) If $r_1 > 1$, then obviously $r_1 > y_2$ and thus $\beta < 1$. Now assume $r_2 > 1$. Then, for $\beta < 1$ we should prove that $r_1 > y_2$. Note that $f(r_1)$ is positive for all values $r_1 \in (0,1)$. This implies that $r_1 < y_1$ or $r_1 > y_2$ (see the proof of Lemma 4.4). Furthermore, $y_1 < \hat{y} < 1/2$ for $r_2 > 1$ and $r_1 \in (0,1)$, when $\hat{y}$ as defined in the proof of Lemma 4.4. Hence, for $r_1 \geq 1/2$ it clearly holds that $r_1 > y_1$. Assume that there exists a value $r_1 \in (0,1)$ for which it holds that $r_1 < y_1$. Then, since y_1 is a continuous function of r_1, there should be a value in $(0,1)$ for which $r_1 = y_1$ and hence $f(r_1) = 0$. This is not the case, and thus $r_1 > y_2$ for all values $r_1 \in (0,1)$. □

We again note that $\beta = 1$ (resp. $\beta < 1$, $\beta > 1$) implies $1 \in R$ (resp. $1 \notin R \cup R^+$, $1 \in R^+$), which plays a crucial role in the numerical work to be presented in Section 8.

5 Boundary value problem I

In the previous section we considered the kernel as a polynomial in either y or x, which may lead to the curves L and R, respectively. In this section we will show how the curve L, derived in Section 4.1, leads to a Riemann-Hilbert boundary value problem for the function $P(0,y)$.

Lemma 5.1. *The function $P(0,y)$ is regular in the domain L^+ and satisfies for $y \in L$ the condition*

$$\mathrm{Im}[P(0,y)] = \mathrm{Im}\Big[- P(0,0)\frac{h_4(r_2|y|^2/r_1, y)}{h_3(r_2|y|^2/r_1, y)}\Big]. \tag{5.1}$$

Proof: For zero-pairs (x,y) of the kernel $h_1(x,y)$ for which $P(x,y)$ is finite we have

$$h_2(x,y)P(x,0) + h_3(x,y)P(0,y) + h_4(x,y)P(0,0) = 0, \tag{5.2}$$

from which it follows that, for those zero-pairs,

$$P(0,y) = \frac{1-p}{p}P(x,0) - \frac{h_4(x,y)}{h_3(x,y)}P(0,0) = 0. \tag{5.3}$$

Thus, (5.1) follows from the fact that $P(x,0)$ is real for $x \in [0,x_2]$ and $|y|^2 = r_1 x/r_2$ for $y \in L$. If $\alpha \leq 1$, L lies entirely within the unit circle. Hence, $P(0,y)$ is regular in L^+. If $\alpha > 1$, $P(0,y(x))$ can be continued analytically over the interval $[0,x_2]$ via (5.2), because $P(x,0)$ is regular on this interval. Hence, the analytic continuation of $P(0,y)$ is finite at $y = y(x_2)$. Because $P(0,y)$ has a power series expansion at $y = 0$ with positive coefficients, this implies that $P(0,y)$ is regular for $|y| < y(x_2)$ and hence in L^+. □

Lemma 5.1 shows that the determination of $P(0,y)$ reduces to the determination of the solution of the following Riemann-Hilbert boundary value problem on the contour L:

Determine a function $P(0,y)$ such that

1. $P(0,y)$ is regular for $y \in L^+$ and continuous for $y \in L^+ \cup L$.
2. $\mathrm{Re}\,[iP(0,y)] = c(y)$, for $y \in L$,

where

$$c(y) = \mathrm{Im}\Big[P(0,0)\frac{h_4(r_2|y|^2/r_1, y)}{h_3(r_2|y|^2/r_1, y)}\Big].$$

5.1 Reduction to a Dirichlet problem on a circle

The standard way to solve this type of boundary value problem is to transform the boundary condition (5.1) to a condition on the unit circle (see e.g. Muskhelishvili [10], p. 108). Denote the unit circle by C and its interior by C^+. We introduce the conformal mapping

$$z = f(y) : L^+ \to C^+, \tag{5.4}$$

and its inverse

$$y = f_0(z) : C^+ \to L^+. \tag{5.5}$$

Using these mappings, we can reduce the Riemann-Hilbert problem on L to the following problem:

Determine a function $G(z)$ such that

1. $G(z)$ is regular for $z \in C^+$ and continuous for $z \in C \cup C^+$.
2. $\mathrm{Re}\,[iG(z)] = \tilde{c}(z)$, for $z \in C$, where $\tilde{c}(z) = c(f_0(z))$,

which is known as the Dirichlet problem on a circle. Its solution is given by (see [10], p. 108)

$$G(z) = \frac{1}{2\pi}\int_C \tilde{c}(w)\frac{w+z}{w-z}\frac{\mathrm{d}w}{w} + K_1, \quad z \in C \cup C^+, \tag{5.6}$$

where K_1 is some constant. In this way, $P(0,y)$ has been formally determined as

$$P(0,y) \;=\; G(f(y)) \;=\; \frac{1}{2\pi}\int_C c(f_0(w))\frac{w+f(y)}{w-f(y)}\frac{\mathrm{d}w}{w} + K_1, \quad y \in L \cup L^+. \tag{5.7}$$

We can rewrite the contour integral (5.7) as a real integral on $[0, x_2]$. That is, for $y \in L^+ \cup L$, we have that

$$\begin{aligned} P(0,y) &= \frac{1}{2\pi}\int_L c(s)\frac{f(s)+f(y)}{f(s)-f(y)}\frac{\mathrm{d}f(s)}{f(s)} + K_1 \\ &= \frac{1}{2\pi}\Big[-\int_0^{x_2} c(y_1(x))\frac{f(y_1(x))+f(y)}{f(y_1(x))-f(y)}\frac{f'(y_1(x))y_1'(x)}{f(y_1(x))}\mathrm{d}x \\ &\quad + \int_0^{x_2} c(y_2(x))\frac{f(y_2(x))+f(y)}{f(y_2(x))-f(y)}\frac{f'(y_2(x))y_2'(x)}{f(y_2(x))}\mathrm{d}x\Big] + K_1. \end{aligned} \tag{5.8}$$

5.2 Mapping $f(y)$

For this specific problem, an explicit expression for the conformal mapping $f(y)$ can be found (see Blanc [2]). It is given by

$$f(y) = \frac{yk(\eta) - \eta k(y)}{yk(\eta) + \eta k(y)}, \tag{5.9}$$

where

$$k(y) = (\alpha - y)\sqrt{r_1 - r_2^2\alpha^2 y},$$

and η is some unspecified constant in the interval $(0, \alpha)$. For our computations we set $\eta = \alpha/2$. With the explicit expression for $f(y)$ we have all ingredients for calculating the integral (5.8), as will be further discussed in Section 8.

6 Boundary value problem II

In this section we will show how the zero-set discussed in Section 4.2 that leads to the curve R gives rise to a Riemann-Hilbert problem for the function $P(x, 0)$. The approach is similar to the one followed in Section 5.

Lemma 6.1. *The function $P(x, 0)$ is regular in the domain R^+ and satisfies for $x \in R$ the condition*

$$\mathrm{Im}[P(x, 0)] = \mathrm{Im}\Big[- P(0, 0)\frac{h_4(x, r_1|x|^2)}{h_2(x, r_1|x|^2)}\Big] \tag{6.1}$$

Proof: Similar to the proof of Lemma 5.1 □

Lemma 6.1 shows that the determination of $P(x, 0)$ reduces to the determination of the solution of the following Riemann-Hilbert boundary value problem on the contour R:

Determine a function $P(x, 0)$ such that

1. $P(x, 0)$ is regular for $x \in R^+$ and continuous for $x \in R \cup R^+$.
2. Re $[iP(x, 0)] = d(x)$, for $x \in R$,

where

$$d(x) = \mathrm{Im}\Big[P(0, 0)\frac{h_4(x, r_1|x|^2)}{h_2(x, r_1|x|^2)}\Big]. \tag{6.2}$$

Note that this problem is inherently different from the Riemann-Hilbert problem for $P(0, y)$ discussed in the previous section, in the sense that there is no symmetry in x and y. Moreover, the contours on which the problems have been defined have different features as well (see Lemma 4.2 and Lemma 4.5).

We introduce the conformal mapping

$$z = g(x) : R^+ \to C^+, \tag{6.3}$$

and its inverse

$$x = g_0(z) : C^+ \to R^+, \tag{6.4}$$

which allows us, as in Section 5.1, to reduce the Riemann-Hilbert problem to the following Dirichlet problem on the unit circle:

Determine a function $H(z)$ such that

1. $H(z)$ is regular for $z \in C^+$ and continuous for $z \in C \cup C^+$.
2. Re $[iH(z)] = \tilde{d}(z)$, for $z \in C$, where $\tilde{d}(z) = d(g_0(z))$.

This implies that the solution of $P(x,0)$ is given by

$$P(x,0) \;=\; H(g(x)) \;=\; \frac{1}{2\pi}\int_C d(g_0(w))\frac{w+g(x)}{w-g(x)}\frac{\mathrm{d}w}{w} + K_2, \quad x \in R \cup R^+, \tag{6.5}$$

where K_2 is some constant.

6.1 Mapping $g_0(z)$

The explicit mapping for $f(y)$ as described in Section 5.2 has been obtained by exploiting the specific properties of L, among which that the contour passes through zero. Unfortunately, we have not been able to derive an exact expression for $g(x)$. The standard approach in these cases is to determine the inverse mapping $g_0(z)$ using a well-known method from the theory of conformal mappings. This is sufficient to calculate (6.5), since we show in Section 8 that we do not need the mapping $g(x)$ to evaluate $P(x,0)$ in x.

For this approach, we need a representation of R in terms of polar coordinates, i.e.

$$R = \{x : x = \rho(\phi)\exp(i\phi),\ 0 \le \phi \le 2\pi\}, \tag{6.6}$$

which can be obtained in the following way. Since $0 \in R^+$, we have by (4.8) that for each point x on R the relation between its absolute value and its real part is given by $|x|^2 = m(\mathrm{Re}(x))$, where

$$m(\delta) := \frac{1}{r_1 r_2(\hat{r} - 2\delta)}. \tag{6.7}$$

So, given the angle ϕ belonging to some point on R, the real part of this point, to be denoted by $\delta(\phi)$, is the solution of

$$\delta - \cos\phi\sqrt{m(\delta)} = 0, \quad 0 \le \phi \le 2\pi. \tag{6.8}$$

One may ask whether the solution to (6.8) is unique. This is the case when R is a Jordan curve for which it holds that every ray from the point 0 intersects the curve R exactly once. In fact, this is the notion of starshapedness (see [12], p.125, Exercise 109). In all cases we have considered, R is a smooth and egg-shaped contour, and thus a starshaped Jordan curve. We see that $\rho(\phi) = \delta(\phi)/\cos\phi$, and so the parametrization in (6.6) is fully specified.

For a contour that can be described in polar coordinates, the mapping from C^+ to the interior of this contour is formally given by (cf. [5], Section I.4.4, [8], Section 2.1):

$$g_0(z) = z\exp[\frac{1}{2\pi}\int_0^{2\pi}\log\{\rho(\theta(\omega))\}\frac{e^{i\omega}+z}{e^{i\omega}-z}\mathrm{d}\omega], \quad |z| < 1, \tag{6.9}$$

with the angular deformation $\theta(\cdot)$ uniquely determined as the solution of Theodorsen's integral equation

$$\theta(\phi) = \phi - \int_0^{2\pi}\log\{\rho(\theta(\omega))\}\cot\{\frac{1}{2}(\omega-\phi)\}\mathrm{d}\omega, \quad 0 \le \phi \le 2\pi. \tag{6.10}$$

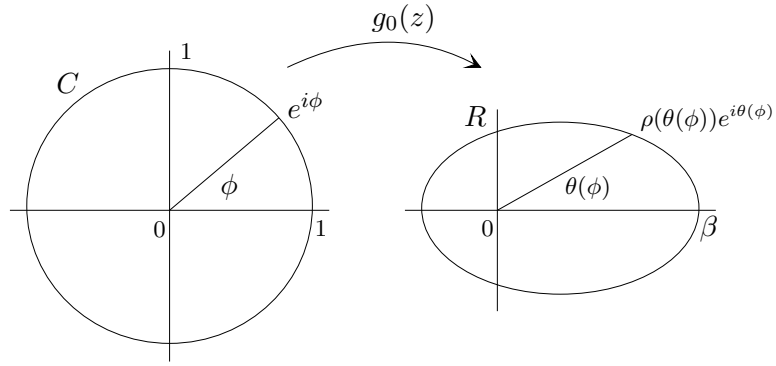

Figure 3: Finding a boundary correspondence point through the mapping $x = g_0(z) : C \to R$.

Here, $\theta(\phi)$ is a strictly increasing and continuous function of ϕ, and $\theta(\phi) = 2\pi - \theta(2\pi - \phi)$. According to the corresponding-boundaries theorem (see [5], p. 66), $g_0(z)$ is continuous in $C \cup C^+$. Equation (6.10) is nonlinear and cannot be solved in closed form, though a unique solution can be proven to exist.

We use (6.10) to determine boundary correspondence points. That is, for a point on the unit circle given by its angle ϕ, we solve (6.10) numerically to obtain the corresponding point on R, given by its angle $\theta(\phi)$, see Figure 3. The numerical issues of this procedure are discussed in Section 8.3.

7 Performance measures

In this section we present exact expressions for two performance measures: the fraction of time a station is empty and the mean stationary queue length at a station. Furthermore, we show for both performance measures that a relation exists between its value at station 1 and station 2. As a consequence, an expression for a performance measure for one of the stations yields the performance measure for the other station as well.

7.1 Fraction of time stations are empty

The fractions of time station 1 and 2 are empty are given by $P(0,1)$ and $P(1,0)$, respectively. Determining either $P(0,1)$ or $P(1,0)$ is sufficient to obtain both, since they are related in the following way. Setting $x = y$ in (3.1) and taking the limit $x \uparrow 1$ gives

$$P(1,0) = 1 - \frac{\lambda}{\nu_2} - \frac{p}{1-p}\Big[1 - \frac{\lambda}{\nu_1} - P(0,1)\Big]. \tag{7.1}$$

Equation (7.1) alternatively follows from one of the equations

$$\begin{aligned}
\lambda &= \nu_1(P(1,0) - P(0,0)) + p\nu_1(1 - P(1,0) - P(0,1) + P(0,0)),\\
\lambda &= \nu_2(P(0,1) - P(0,0)) + (1-p)\nu_2(1 - P(1,0) - P(0,1) + P(0,0)).
\end{aligned}$$

These equations stem from the following reasoning: $P(1,0) - P(0,0)$ is the fraction of time station 1 is nonempty while station 2 is empty, and $1 - P(1,0) - P(0,1) + P(0,0)$ is the fraction of time both stations are nonempty. Thus, the first equation states that, for station 1, the arrival rate equals the departure rate. Similarly, the second equation corresponds to the equality of arrival-departure rates for station 2.

7.2 Mean queue lengths

We will now derive expressions for the mean queue length at both stations, to be denoted by $\mathbb{E}X_1$ and $\mathbb{E}X_2$. First, we show how these mean queue lengths are related. Differentiating both sides of (3.2) w.r.t. y, and letting $y \uparrow 1$, yields

$$\mathbb{E}X_1\Big[\frac{1}{\nu_1}+\frac{1}{\nu_2}\Big]+\mathbb{E}X_2\frac{1}{\nu_2}=\frac{\lambda(\nu_1^2+\nu_1\nu_2+\nu_2^2)}{\nu_1\nu_2(\nu_1\nu_2-\lambda(\nu_1+\nu_2))}. \tag{7.2}$$

Again, an interpretation can be given. The left-hand side of (7.2) counts the mean amount of work in the system by multiplying the mean number of jobs at each station by the mean service time they still require. The right-hand side of (7.2) corresponds to the mean amount of work in an $M/G/1$ queue (see e.g. [4]), with Poisson arrivals with rate λ and service times distributed as the sum of two exponentially distributed random variables with mean $1/\nu_1$ and $1/\nu_2$, respectively. Both sides of (7.2) are equal due to the work conservation property of the system. By (7.2) it suffices to calculate either $\mathbb{E}X_1$ or $\mathbb{E}X_2$ to obtain them both. We will show how $\mathbb{E}X_2$ and $\mathbb{E}X_1$ follow from the solution of the Riemann-Hilbert boundary value problems discussed in Section 5 and 6, respectively.

When setting $x=1$ in (3.1), the factor $(y-1)$ cancels from all terms leaving

$$P(1,y)=\frac{\nu_1 y+\nu_2}{p\nu_1 y-(1-p)\nu_2}(-(1-p)P(1,0)+pP(0,y))+\frac{(1-p)\nu_1 y-p\nu_2}{p\nu_1 y-(1-p)\nu_2}P(0,0). \tag{7.3}$$

Taking derivatives w.r.t. y at both sides of (7.3) yields

$$\begin{aligned}\frac{d}{dy}P(1,y) &= \frac{\nu_1\nu_2}{(p\nu_1 y-(1-p)\nu_2)^2}((1-p)P(1,0)-pP(0,y))\\ &\quad+\frac{(\nu_1 y+\nu_2)p}{p\nu_1 y-(1-p)\nu_2}\,\frac{d}{dy}P(0,y)+\frac{(2p-1)\nu_1\nu_2 P(0,0)}{(p\nu_1 y-(1-p)\nu_2)^2}.\end{aligned} \tag{7.4}$$

Plugging (7.1) into (7.4) and setting $y=1$ then gives for $p\nu_1\neq(1-p)\nu_2$:

$$\mathbb{E}X_2=\Big[\frac{d}{dy}P(1,y)\Big]_{y=1}=-\frac{\lambda}{p\nu_1-(1-p)\nu_2}+\frac{(\nu_1+\nu_2)p}{p\nu_1-(1-p)\nu_2}\Big[\frac{d}{dy}P(0,y)\Big]_{y=1}. \tag{7.5}$$

Thus, to determine $\mathbb{E}X_2$, we only need to compute $[\frac{d}{dy}P(0,y)]_{y=1}$. Note that from (5.7) we have that

$$\frac{d}{dy}P(0,y)=\frac{1}{\pi}\int_C c(f_0(w))\frac{f'(y)}{(w-f(y))^2}\mathrm{d}w. \tag{7.6}$$

Similarly, when setting $y=1$ in (3.1), the factor $(x-1)$ cancels from all terms, which gives

$$P(x,1)=\frac{(1-p)\nu_1}{p\nu_1-\lambda x}\Big[\frac{p}{1-p}P(0,1)-P(x,0)+P(0,0)\Big] \tag{7.7}$$

Taking derivatives w.r.t. x at both sides of (7.7) yields

$$\begin{aligned}\frac{d}{dx}P(x,1) &= \frac{\lambda\nu_1(1-p)}{(p\nu_1-\lambda x)^2}\Big[\frac{p}{1-p}P(0,1)-P(x,0)+P(0,0)\Big]\\ &\quad-\frac{(1-p)\nu_1}{p\nu_1-\lambda x}\,\frac{d}{dx}P(x,0).\end{aligned} \tag{7.8}$$

Plugging (7.1) into (7.8) and letting $x = 1$ then gives for $\lambda \neq p\nu_1$:

$$\mathbb{E}X_1 = \left[\frac{d}{dx}P(x,1)\right]_{x=1} = \frac{\lambda}{p\nu_1 - \lambda} - \frac{(1-p)\nu_1}{p\nu_1 - \lambda}\left[\frac{d}{dx}P(x,0)\right]_{x=1}. \tag{7.9}$$

Note that from (6.5) we have that

$$\frac{d}{dx}P(x,0) = \frac{1}{\pi}\int_C d(g_0(w))\frac{g'(x)}{(w-g(x))^2}\mathrm{d}w. \tag{7.10}$$

Remark 7.1. When $p\nu_1 = (1-p)\nu_2$, setting $y = 1$ in (7.3) gives (after applying l'Hôpital)

$$\left[\frac{d}{dy}P(0,y)\right]_{y=1} = \frac{\lambda}{(\nu_1+\nu_2)p} = \frac{\lambda}{\nu_2}.$$

We then have an exact expression for $[\frac{d}{dy}P(0,y)]_{y=1}$, but we cannot use (7.5) to determine $\mathbb{E}X_2$. We can, though, use (7.9) to find $\mathbb{E}X_1$, and $\mathbb{E}X_2$ through (7.2), since λ is always smaller than $p\nu_1$ (when $p\nu_1 = (1-p)\nu_2$) due to the ergodicity condition (2.1). Likewise, for $\lambda = p\nu_1$, setting $x = 1$ in (7.7) gives (after applying l'Hôpital)

$$\left[\frac{d}{dx}P(x,0)\right]_{x=1} = \frac{\lambda}{(1-p)\nu_1} = \frac{\lambda}{\nu_1 - \lambda},$$

and we cannot use (7.9) to determine $\mathbb{E}X_1$. We can use (7.5) to find $\mathbb{E}X_2$, since $(1-p)\nu_2$ is always smaller than $p\nu_1$ (when $\lambda = p\nu_1$) due to the ergodicity condition. We can thus conclude that we can calculate either one of the integrals (7.6) or (7.10) for all allowed parameter values.

8 Computational issues

We will now discuss some issues that arise when numerically determining the performance measures from the formal solutions of the Riemann-Hilbert boundary value problems. In Section 8.1 we discuss how the location of α and β is related to the set of parameter values for which we can actually determine the performance measures. In Section 8.2 we discuss a way to determine the performance measures for all allowed parameter values. In Section 8.3 we discuss how the integrals involved in calculating the performance measures can be determined numerically.

8.1 Remarks on α and β

For calculating the performance measures described in Section 7, we have to evaluate $P(0,y)$ and $\frac{d}{dy}P(0,y)$ in $y = 1$ or $P(x,0)$ and $\frac{d}{dx}P(x,0)$ in $x = 1$. We first discuss the first option.

The integration constant K_1 can be determined by calculating $P(0,0)$ from the integral (5.7), and using that $P(0,0) = 1 - \lambda/\nu_1 - \lambda/\nu_2$. The integrals (5.7), (7.6), however, follow from the solution of a Dirichlet problem that is only defined on or within the unit circle. So, in order to evaluate the integrals, $f(1)$ should lie on or within the unit circle, which is the same as requiring 1 to lie on or within the contour L.

The above problem is very common in queueing applications for which the boundary value technique is applied (see e.g. Boxma & Groenendijk [3], Cohen & Boxma [5], p. 360, De Klein [9], p. 89, and Feng et al. [7]). In the current application, a key role is played by

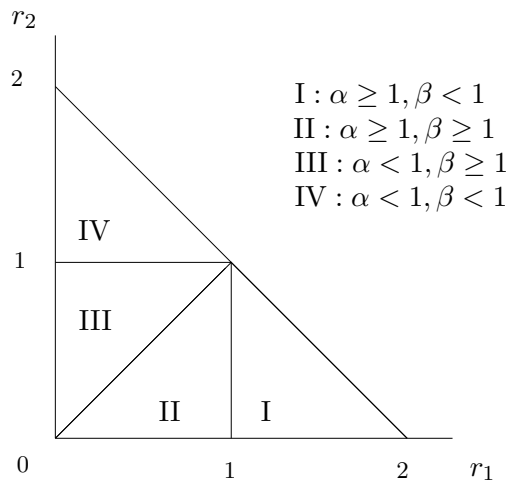

Figure 4: Relation between parameter values, and α and β, for $p = \frac{1}{2}$.

α. In Lemma 4.3 we saw that, when $p\nu_1 \leq (1-p)\nu_2$ (i.e. $r_1 \geq r_2$), it follows that $\alpha \geq 1$ and thus $1 \in L \cup L^+$. Hence, for these parameter values the integrals (5.7), (7.6) can be calculated. To obtain results for parameter values for which it holds that $p\nu_1 > (1-p)\nu_2$, we might consider analytic continuations for the functions (5.7), (7.6), see e.g. Nauta [11]. However, this would most probably result in numerical difficulties. Alternatively, we can use Taylor series expansion of the corresponding functions around some point in L^+, as suggested by Cohen & Boxma [5], p. 360. For a Taylor series expansion of order n around $\hat{y} \in L^+$, we then have that

$$P(0,1) \approx \sum_{k=0}^{n} \frac{(1-\hat{y})^k}{k!} \Big[\frac{d^k}{dy^k} P(0,y)\Big]_{y=\hat{y}}. \tag{8.1}$$

The exact same problem holds for boundary value problem II. In that case, we have to evaluate the integrals (6.5), (7.10) in $x = 1$, which is only allowed when $1 \in R \cup R^+$. In Lemma 4.6 we have seen that this is the case when $p\nu_1$ and $(1-p)\nu_2$ are both larger than λ (i.e. $r_1 < 1$ and $r_2 < 1$).

To summarize things, we show in Figure 4 how the values of α and β are related to the parameter values λ, ν_1, ν_2 (for $p = 1/2$). So, starting from boundary value problem I, we can determine the performance measures for parameter values that fall within area I and II. By considering boundary value problem II, we can enlarge this set by area III. For area IV we can apply the Taylor series expansion. As will be shown in the next section using the Taylor series expansion can be circumvented by considering a third zero-set of the kernel $h_1(x,y)$.

8.2 A third zero-set of the kernel

We now discuss an approach to determine $P(0,1)$ and $\frac{d}{dy}P(0,y)|_{y=1}$ directly from (5.7), (7.6) despite the fact that $\alpha < 1$. The approach has been suggested by De Klein [9], p. 89, and makes use of a zero-set of $h_1(x,y)$ other than the one in Section 4.1. By establishing a relation between $P(x,0)$ and $P(0,y)$ for zero-pairs (x,y) of this set, we are able to calculate the performance measures for all allowed parameter values.

The new zero-set is defined by

$$\{(x, y^*(x)) \mid h_1(x, y^*(x)) = 0, |x| = 1\}, \tag{8.2}$$

where $y^*(x)$ is the zero of the kernel with the smallest modulus. From the function $y(x)$, as given in (4.2), it is easily seen that

$$y^*(1) = \min\Big\{\frac{r_1}{r_2}, 1\Big\}, \tag{8.3}$$

for which we have the following result:

Lemma 8.1. *For $r_1 = r_2$ it holds that $y^*(1) = 1 = \alpha$. For $r_1 \neq r_2$ it holds that $y^*(1) < \alpha$.*

Proof: The first assertion follows immediately from Lemma 4.3. For the second assertion note that if $r_1 > r_2$ it holds that $y^*(1) = 1 < \alpha$. If $r_1 < r_2$ it holds that

$$D_1(r_1/r_2) = \Big[1 + r_1 + \frac{r_1}{r_2} - \frac{r_1^2}{r_2}\Big]^2\Big(\frac{1}{r_2}\Big)^2 - 4\Big(\frac{1}{r_2}\Big)^2.$$

Since $r_1 < r_2$ implies that $r_1 < 1$, we have that $1 + r_1 + r_1/r_2 - r_1^2/r_2 \in (-2, 2)$, and $D_1(r_1/r_2) < 0$. So, $r_1/r_2 < x_2$, and thus $y^*(1) = r_1/r_2 < \sqrt{r_1 x_2/r_2} = \alpha$. □

We exploit the result in Lemma 8.1 in the following way. Introducing the short-hand notation $h_k(x) := h_k(x, y^*(x))$, we obtain from (3.1) that

$$h_2(x)P(x, 0) + h_3(x)P(0, y^*(x)) + h_4(x)P(0, 0) = 0, \quad |x| = 1. \tag{8.4}$$

Setting $x = 1$ in (8.4) yields

$$P(1, 0) = \frac{-1}{h_2(1)}\Big[h_3(1)P(0, y^*(1)) + h_4(1)P(0, 0)\Big]. \tag{8.5}$$

Since for $r_1 \neq r_2$ it holds that $y^*(1) < \alpha$, the value of $P(0, y^*(1))$ can be computed directly from (5.7). Hence, for $r_1 < r_2$ we cannot obtain $P(0, 1)$ directly from (5.7), but we can obtain $P(1, 0)$ using (5.7), and find $P(0, 1)$ through (7.1).

By using a similar approach we can determine $[\frac{d}{dy}P(0, y)]_{y=1}$ through (7.6), despite the fact that $r_1 < r_2$. We do need some extra results concerning the zero-set (8.2) though. Observe that $y^*(1)$ is of multiplicity 1 unless $r_1 = r_2$ (for which $y^*(1)$ is of multiplicity two). We further have

Lemma 8.2. *The zero $y^*(x)$ is of multiplicity 1 and contained in the disk $|y| < 1$ for every $|x| = 1$, $x \neq 1$.*

Proof: For $|x| = 1$ it holds that $h_1(x, y) = \lambda x(f(y) + g(y))$ where

$$f(y) := (1 + \frac{1}{r_1} + \frac{1}{r_2} - x)y, \quad g(y) := -\Big(\frac{1}{r_1}\bar{x}y^2 + \frac{1}{r_2}\Big),$$

and $\bar{x}$ the complex conjugate of x. We have for $|x| = 1$, $x \neq 1$,

$$\begin{aligned} |f(y)| &= |1 + \frac{1}{r_1} + \frac{1}{r_2} - x||y| > \Big(\frac{1}{r_1} + \frac{1}{r_2}\Big)|y|, \\ |g(y)| &\leq \frac{1}{r_1}|\bar{x}||y|^2 + \frac{1}{r_2} = \frac{1}{r_1}|y|^2 + \frac{1}{r_2}. \end{aligned}$$

Then, for all points y on $|y| = 1$ we have that

$$|g(y)| \leq \frac{1}{r_1} + \frac{1}{r_2} < |f(y)|, \quad |y| = 1,\ |x| = 1,\ x \neq 1,$$

which implies by Rouché's theorem (see e.g. Cohen [4], p. 652) that $f(y) + g(y)$ (and thus $h_1(x, y)$) has as many zeros (counted according to there multiplicity) inside $|y| = 1$ as $f(y)$. Since $f(y)$ has only one zero of multiplicity 1 at $y = 0$, we find that for every x with $|x| = 1,\ x \neq 1$, $h_1(x, y) = 0$ has one solution inside $|y| = 1$, i.e. $y^*(x)$. □

From Lemma 8.2 it follows for $r_1 \neq r_2$ and $|x| = 1$ that

$$\Big[\frac{d}{dy} h_1(x, y)\Big]_{y=y^*(x)} \neq 0, \tag{8.6}$$

because otherwise $y^*(x)$ would be of multiplicity 2. From the implicit function theorem we then have that $y^*(x)$ is differentiable for $r_1 \neq r_2$ and $|x| = 1$. Differentiating $h_1(x, y^*(x)) = 0$ at both sides then gives

$$\Big[\frac{d}{dx} h_1(x, y)\Big]_{y=y^*(x)} + \frac{d}{dx} y^*(x) \Big[\frac{d}{dy} h_1(x, y)\Big]_{y=y^*(x)} = 0, \tag{8.7}$$

and thus

$$\frac{d}{dx} y^*(x) = -\frac{\Big[\frac{d}{dx} h_1(x, y)\Big]_{y=y^*(x)}}{\Big[\frac{d}{dy} h_1(x, y)\Big]_{y=y^*(x)}}. \tag{8.8}$$

Consequently, differentiating (8.4) w.r.t. x and setting $x = 1$ gives

$$\begin{aligned} \Big[\frac{d}{dx} P(x, 0)\Big]_{x=1} &= \frac{-1}{h_2(1)} \Big(h_2'(1) P(1, 0) + h_3'(1) P(0, y^*(1)) + h_4'(1) P(0, 0) \\ &\quad + h_3(1) \Big[\frac{d}{dx} y^*(x)\Big]_{x=1} \Big[\frac{d}{dy} P(0, y)\Big]_{y=y^*(1)} \Big). \end{aligned} \tag{8.9}$$

Again, since for $r_1 \neq r_2$ it holds that $y^*(1) < \alpha$, the value of $[\frac{d}{dy} P(0, y)]_{y=y^*(1)}$ can be computed directly from (7.6), and $P(0, 1)$ can be computed from (8.5) and (7.1). The approach outlined in this section can also be applied to determine $P(1, 0)$ and $[\frac{d}{dx} P(x, 0)]_{x=1}$ in case $\beta < 1$.

8.3 Evaluating the integrals

We will now describe how the involved integrals can be determined numerically. For boundary value problem I, we have rewritten the integral (5.7) as (5.8). The integral (7.6) can be rewritten in a similar way. We will evaluate the integrals (5.8) and (7.6) using the trapezium rule, for which we split the interval $[0, 2\pi]$ into K parts of equal length $2\pi/K$. The fact that the whole integrand including the mapping $f(y)$ is known explicitly allows for a fine subdivision. For the numerical results to be presented in the next section we have set K to 250.

For boundary value problem II, we should calculate the integrals (6.5) and (7.10). We will now outline how these integrals can be computed, along with the numerical determination

of the mapping $g_0(z)$ that was introduced in Section 6.1. For a more detailed exposition we refer to Chapter IV.1 of [5].

Step 1: Rewriting the integrals (6.5) *and* (7.10)
Substitution of $w = e^{i\phi}$ into (6.5) yields

$$P(x,0) = \frac{i}{2\pi}\int_0^{2\pi} d(g_0(e^{i\phi}))\frac{e^{i\phi}+g(x)}{e^{i\phi}-g(x)}\mathrm{d}\phi + K_2, \quad x \in R \cup R^+. \tag{8.10}$$

The integral (7.10) can be rewritten in a similar way, i.e.

$$\frac{d}{dx}P(x,0) = \frac{i}{\pi}\int_0^{2\pi} d(g_0(e^{i\phi}))\frac{g'(x)e^{i\phi}}{(e^{i\phi}-g(x))^2}\mathrm{d}\phi, \quad x \in R \cup R^+. \tag{8.11}$$

Step 2: Numerical evaluation of the integrals (8.10) *and* (8.11)
We will evaluate the integrals (8.10) and (8.11) in $x = 1$ using the above rewriting and the trapezium rule, for which we split the interval $[0, 2\pi]$ into K parts of equal length $2\pi/K$. From (8.10) and (8.11) we then see that we need to determine the values of the conformal mapping $g_0(\cdot)$ in the points $e^{i\phi_k},\ k = 0, 1, \ldots, K-1$, with $\phi_k = 2\pi k/K$. We further need to determine $g(1)$ and $g'(1)$.

Step 3: Solving Theodorsen's integral equation (6.10)
For K points on the unit circle given by their angles $\{\phi_1, \phi_2, \ldots, \phi_K\}$, we should solve (6.10) to obtain the corresponding points on R, given by their angles $\{\theta(\phi_1), \theta(\phi_2), \ldots, \theta(\phi_K)\}$. Thereto, we determine $\theta(\phi_k),\ k = 0, 1, \ldots, K-1$, iteratively (see Gaier [8], p. 67), from

$$\theta_0(\phi_k) = \phi_k, \tag{8.12}$$

$$\theta_{n+1}(\phi_k) = \phi_k - \int_0^{2\pi} \log\{\frac{\delta(\theta_n(\omega))}{\cos(\theta_n(\omega))}\}\cot\{\frac{1}{2}(\omega-\phi_k)\}\mathrm{d}\omega, \tag{8.13}$$

where $\delta(\theta_n(\omega))$ is determined from (see (6.8))

$$\delta(\theta_n(\omega)) - \cos\theta_n(\omega)\sqrt{m(\delta(\theta_n(\omega)))} = 0, \tag{8.14}$$

using the Newton-Raphson root-finding procedure. For each step, the integral in (8.13) is numerically determined by again using the trapezium rule with K parts of equal length $2\pi/K$. For the iteration, we have used the following stopping criterion:

$$\max_{k\in\{0,\ldots,K-1\}} |\theta_{n+1}(\phi_k) - \theta_n(\phi_k)| < 10^{-6}. \tag{8.15}$$

Finally, it follows from $\rho(\phi) = \delta(\phi)/\cos\phi$ that the value of $g_0(\cdot)$ in $e^{i\phi_k}$ is given by

$$g_0(e^{i\phi_k}) = \frac{\delta(\theta(\phi_k))}{\cos\theta(\phi_k)}e^{i\theta(\phi_k)}, \quad k = 0, 1, \ldots, K-1. \tag{8.16}$$

For the numerical results to be presented in the next section we have set K to 250.

Step 4: Determination of $g(1)$ and $g'(1)$
$g(1)$ is obtained as the unique solution z of $g_0(z) = 1$ on $[0, 1]$, and can be determined using (6.9) and Newton-Raphson. $g'(1)$ is given by (see Boxma & Groenendijk [3])

$$g'(1) = \Big[\frac{1}{g(1)} + \frac{1}{2\pi}\exp[\frac{1}{2\pi}\int_0^{2\pi}\log\{\frac{\delta(\theta(\omega))}{\cos(\theta(\omega))}\}\frac{2e^{i\omega}}{(e^{i\omega}-g(1))^2}\mathrm{d}\omega]\Big]^{-1}. \tag{8.17}$$

We calculate $g'(1)$ by numerically determining the integral (8.17) with the trapezium rule and K set to 250.

9 Numerical results

In this section we present some numerical results. In Section 8 we have concluded that we can determine the performance measures for the whole set of parameter values $\{\lambda, \nu_1, \nu_2, p\}$ for which the ergodicity condition (2.1) is satisfied. Moreover, as we have seen in Sections 8.1 and 8.2, part of this set allows for multiple ways to determine the performance measures. Therefore, we explicitly mention that for all results presented in this section that could be obtained in more than one way, we checked upon the different ways to generate the same result (to at least two decimals).

Table 1: Performance measures for an average load incurred to the system.

λ	ν_1	ν_2	p	r_1	r_2	α	β	$P(1,0)$	$P(0,1)$	$\mathbb{E}X_1$	$\mathbb{E}X_2$
1	3	3	0.00	∞	0.33	-	-	0.44	0.67	1.33	0.33
1	3	3	0.25	1.33	0.44	1.32	0.86	0.47	0.60	1.25	0.50
1	3	3	0.50	0.67	0.67	1.00	1.15	0.52	0.52	1.02	0.97
1	3	3	0.75	0.44	1.33	0.44	0.86	0.60	0.47	0.68	1.63
1	3	3	1.00	0.33	∞	-	-	0.67	0.44	0.50	2.00
1	6	2	0.00	∞	0.50	-	-	0.50	0.50	1.25	0.50
1	6	2	0.25	0.67	0.67	1.00	1.15	0.61	0.43	0.76	1.16
1	6	2	0.50	0.33	1.00	0.46	1.00	0.73	0.40	0.38	1.67
1	6	2	0.75	0.22	2.00	0.17	0.70	0.80	0.39	0.26	1.83
1	6	2	1.00	0.17	∞	-	-	0.83	0.39	0.20	1.90
1	2	6	0.00	∞	0.17	-	-	0.39	0.83	1.58	0.17
1	2	6	0.25	2.00	0.22	1.57	0.70	0.39	0.80	1.57	0.22
1	2	6	0.50	1.00	0.33	1.37	1.00	0.40	0.73	1.54	0.34
1	2	6	0.75	0.67	0.67	1.00	1.15	0.43	0.61	1.42	0.83
1	2	6	1.00	0.50	∞	-	-	0.50	0.50	1.00	2.50

Table 1 displays the performance measures for an average load incurred to the system. The results for the limiting cases $p = 0$ and $p = 1$ are obtained with the solutions as given in [13]. Obvious observations are that the fraction of time station one is busy, and the mean queue length at station 1, both decrease for higher values of p, and vice versa for station 2. Further note that $\mathbb{E}X_1 + \mathbb{E}X_2$ increases as a function of p. Table 2 displays the performance measures for a high load incurred to the system, from which similar conclusions can be drawn.

For procedures that require two sequential stages, balancing either the mean queue length or the mean workload might be of interest (see e.g. [1]). In Table 1 and 2 we see that the difference in mean queue lengths at the two stations is highly influenced by p. As an example, we have plotted in Fig. 5 both mean queue lengths for $\lambda = 1, \nu_1 = 6, \nu_2 = 2$, and p running

Table 2: Performance measures for a high load incurred to the system.

λ	ν_1	ν_2	p	r_1	r_2	α	β	$P(1,0)$	$P(0,1)$	$\mathbb{E}X_1$	$\mathbb{E}X_2$
1.8	4	4	0.00	∞	0.45	-	-	0.15	0.55	6.53	0.45
1.8	4	4	0.25	1.80	0.60	1.22	0.75	0.16	0.42	6.34	0.82
1.8	4	4	0.50	0.90	0.90	1.00	1.04	0.22	0.22	4.63	4.23
1.8	4	4	0.75	0.60	1.80	0.41	0.75	0.42	0.16	1.42	10.66
1.8	4	4	1.00	0.45	∞	-	-	0.55	0.15	0.82	11.86
1.8	6	3	0.00	∞	0.60	-	-	0.16	0.40	6.60	0.60
1.8	6	3	0.25	1.20	0.80	1.09	0.90	0.20	0.23	5.78	1.83
1.8	6	3	0.50	0.60	1.20	0.60	0.90	0.45	0.15	1.31	8.53
1.8	6	3	0.75	0.40	2.40	0.23	0.65	0.61	0.13	0.64	9.54
1.8	6	3	1.00	0.30	∞	-	-	0.70	0.13	0.43	9.86
1.8	3	6	0.25	∞	0.30	-	-	0.13	0.70	6.90	0.30
1.8	3	6	0.25	2.40	0.40	1.38	0.65	0.13	0.61	6.85	0.82
1.8	3	6	0.50	1.20	0.60	1.19	0.90	0.15	0.45	6.67	4.23
1.8	3	6	0.75	0.80	1.20	0.73	0.90	0.23	0.20	3.57	10.26
1.8	3	6	0.25	0.60	∞	-	-	0.40	0.16	1.50	16.38

from 0 to 1. The imbalance is minimal when $\mathbb{E}X_1 = \mathbb{E}X_2$, i.e. $p \approx 0.18$. Observe that the optimal value of p does not correspond to the solution of $p\nu_1 = (1-p)\nu_2$, which would be 0.25 in this case.

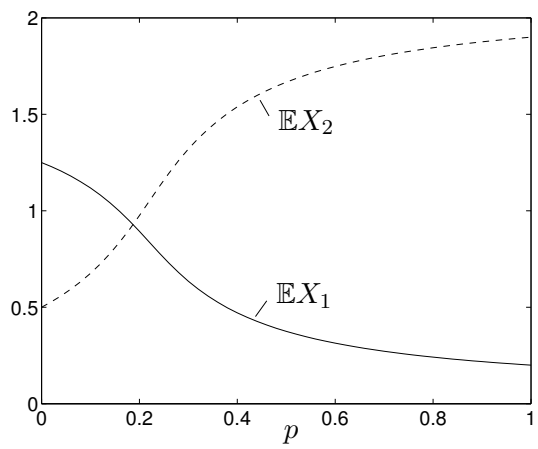

Figure 5: Mean queue lengths for $\lambda = 1, \nu_1 = 6, \nu_2 = 2$, and $p \in [0,1]$.

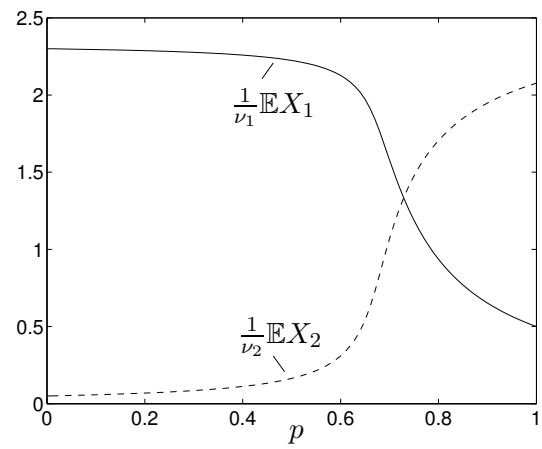

Figure 6: Mean workloads for $\lambda = 1.8, \nu_1 = 3, \nu_2 = 6$, and $p \in [0,1]$.

An example of the influence of p on the mean workloads $\frac{1}{\nu_1}\mathbb{E}X_1$ and $\frac{1}{\nu_2}\mathbb{E}X_2$ is given by Fig. 6, which depicts the mean workloads for $\lambda = 1.8, \nu_1 = 3, \nu_2 = 6$, and p running from 0 to 1. We observe that the imbalance in workloads is minimal when $\frac{1}{\nu_1}\mathbb{E}X_1 = \frac{1}{\nu_2}\mathbb{E}X_2$, i.e. $p \approx 0.72$.

References

[1] S. Andradottir, H. Ayhan and D. Down. Server assignment policies for maximizing the steady-state throughput of finite state queueing systems. *Management Science*, 47:1421-1439, 2001.

[2] J.P.C. Blanc. The relaxation time of two queueing systems in series. *Stochastic Models*, 1:1-16, 1985.

[3] O.J. Boxma and W.P. Groenendijk. Two queues with alternating service and switching times. In *Queueing Theory and its Applications, Liber Amicorum for J.W. Cohen* (eds. O.J. Boxma and R. Syski), p. 261-282, 1988.

[4] J.W. Cohen. *The Single Server Queue*. North-Holland, Amsterdam, 1982.

[5] J.W. Cohen and O.J. Boxma. *Boundary Value Problems in Queueing System Analysis*. North-Holland, Amsterdam, 1983.

[6] G. Fayolle and R. Iasnogorodski. Two coupled processors: The reduction to a Riemann-Hilbert problem. *Zeitschrift für Wahrscheinlichkeitstheorie und Verwandte Gebiete*, 47:325–351, 1979.

[7] W. Feng, M. Kowada and K. Adachi. A two-queue model with Bernouilli service schedule and switching times. *Queueing Systems*, 30:405–434, 1998.

[8] D. Gaier. *Konstruktive Methoden der Konformen Abbildung*. Springer-Verlag, Berlin, 1964.

[9] S.J. de Klein. *Fredholm Integral Equations in Queueing Analysis*. Ph.D. thesis, Rijksuniversiteit Utrecht, 1988.

[10] N.I. Muskhelishvili. *Singular Integral Equations*. Dover Publications, New York, 1992.

[11] H. Nauta. *Ergodicity Conditions for a Class of Two-dimensional Queueing Problems*. Ph.D. thesis, Rijksuniversiteit Utrecht, 1988.

[12] G. Pólya and G. Szegö (1972). *Problems and Theorems in Analysis. Volume I*. Springer-Verlag, New York.

[13] J. Resing and L. Örmeci. A tandem queueing model with coupled processors. *Operations Research Letters*, 31:383–389, 2003.